

Direct simulation Monte Carlo calculations of rarefied flows with incomplete surface accommodation

By R. G. LORD

Oxford University, Department of Engineering Science, Parks Road, Oxford, UK

(Received 3 July 1991 and in revised form 16 January 1992)

Effects of incomplete surface accommodation in rarefied gas flows have been studied using the direct simulation Monte Carlo (DSMC) method in conjunction with the Cercignani–Lampis gas–surface interaction model. Two different flows have been studied, both of which have previously been simulated in DSMC calculations for the case of complete surface accommodation. These are (a) the flow over a sharp, slender circular cone at Mach 5.1 and (b) the flow over a flat-faced circular cylinder at Mach 25. In each case, the gas simulated was nitrogen. It was found that in case (a) the accommodation coefficient of the kinetic energy due to the tangential component of velocity has the greatest influence, whereas in case (b) that of the normal component is also important, having a drastic effect on the rarefied flow field.

1. Introduction

The direct simulation Monte Carlo (DSMC) method (Bird 1976) has become an important means of analysis of rarefied gas flows, on account of its ability to handle complex flow geometries, energy exchange in inelastic inter-molecular collisions, dissociation, ionization and chemical reactions. Much effort has been devoted towards developing realistic models of inter-molecular collision processes (Harvey 1989; Marriott & Harvey 1991; Boyd 1990, 1991).

By comparison, the equally important problems of accurate simulation of interactions between the gas molecules and the solid boundaries of the flow have been largely neglected, most DSMC calculations to date having assumed completely diffuse reflection and complete energy accommodation of gas molecules at solid surfaces. Molecular beam studies and direct measurements of accommodation show, however, that this model is unrealistic, except for highly contaminated surfaces. Molecules re-emitted from clean surfaces show lobular distributions in direction and both energy and momentum accommodation coefficients can be very low. Surfaces of vehicles in space or earth orbit will become gradually decontaminated and it is likely that the consequent reduction in accommodation will have significant effects on aerodynamic forces and heat transfer rates during re-entry.

Of the phenomenological models which have been proposed to describe gas–surface interactions, that of Cercignani & Lampis (1971) (the C–L model), whilst not entirely satisfactory, appears to be the most successful (Cercignani 1971). It satisfies detailed balance (reciprocity) (Kuscer 1971, 1974), produces physically realistic distributions of direction and energy of re-emitted molecules and provides a continuous spectrum of behaviour from specular reflection at one end to diffuse reflection with complete energy accommodation at the other. The model does not, however, include the

important case of diffuse-elastic scattering, i.e. completely diffuse scattering with zero energy accommodation.

Surprisingly, the C-L model has not yet been incorporated into DSMC calculations of rarefied flows, although it has been used in conjunction with other numerical methods (Babovsky *et al.* 1989; Cercignani & Frezzotti 1989). Lord (1991) has shown that it is highly suitable for use in Monte Carlo simulations and that it can also be used to account for classical internal degrees of freedom of the gas molecule, which were not considered in the original formulation of the model.

For the purposes of the present investigation, an existing two-dimensional DSMC program developed by Harvey and his co-workers was used, after modification to incorporate the C-L kernel. Two different flows were studied, both of which had previously been simulated in DSMC calculations for the case of complete surface accommodation. These are (a) the flow over a sharp, slender circular cone at Mach 5.1 and (b) the flow over a flat-ended circular cylinder at Mach 25. The gas simulated was nitrogen in each case and a single molecular collision model, the Morse potential-restricted exchange, variable ϕ model (Davis *et al.* 1983) was used. For each flow, a rather rarefied case, with a free-stream Knudsen number Kn (based on radius) of about 2, and a case much closer to continuum conditions, with $Kn \approx 0.04$, were chosen. In each case, the surface temperature was well below the stagnation temperature of the flow, in order to allow the effects of incomplete accommodation on heat transfer to be studied. Precise values of the various parameters were chosen to coincide, as far as possible, with those of previous simulations. Full details of the flow conditions for both cases are given in Tables 1 and 2. The simulations were all run on the VAX cluster of the Oxford University Computing Service and all required less than one hour's CPU time. The number of timesteps per simulation varied between 3000 and 4680.

No attempt has been made to compare the results of the present calculations with such experimental results as exist. Most of these have been obtained in wind-tunnel environments where no control of surface condition is possible and surfaces would be expected to be highly contaminated and to exhibit virtually complete accommodation. This view is supported by the generally good agreement between experimental results and those of previous simulations which have assumed complete surface accommodation. Moreover, in most cases the scatter of the calculated and experimental data is such as to preclude any definite conclusions as to the merits of the various intermolecular collision models, let alone gas-surface interaction models. The relatively few experiments in which effects of incomplete accommodation appear significant have all used helium rather than nitrogen as test gas, but nitrogen is more realistic for re-entry flows.

2. The Cercignani-Lampis model

It is a property of the C-L model that the three velocity components of the molecule behave independently in a collision with the surface. The two adjustable parameters appearing in the model are actual accommodation coefficients, namely those for the kinetic energy associated with the normal and tangential components of velocity. We shall denote these coefficients by α_n and α_t respectively. (Note, however that Cercignani & Lampis use the symbol α_t for the accommodation coefficient of the tangential momentum of the molecule, which we shall call σ). The model requires that the accommodation coefficients α_t and σ be related by the equation $\alpha_t = \sigma(2 - \sigma)$, and thus that $\sigma < \alpha_t$ (assuming that σ lies between 0 and 1).

$M = 5.09, T_\infty = 84.6 \text{ K}, T_w = 293.2 \text{ K}$
 Incident mass flow rate (units of $\pi R^2 \rho_\infty U_\infty$)

Kn_R	$\alpha = 1$	$\alpha_t = 0.75$	$\alpha_n = 0.75$	$\alpha_r = 0.75$
0.04	0.738	0.754	0.732	0.721
2.00	1.263	1.257	1.297	1.281
(Calculated FM)	1.255	1.255	1.255	1.255

Drag (units of $\frac{1}{2}\pi R^2 \rho_\infty U_\infty^2$)

Kn_R	$\alpha = 1$	$\alpha_t = 0.75$	$\alpha_n = 0.75$	$\alpha_r = 0.75$
0.04	0.774	0.596	0.764	0.763
2.00	2.380	1.362	2.418	2.392
(Calculated FM)	2.652	1.411	2.645	2.652

Heat transfer rate (units of $\frac{1}{2}\pi R^2 \rho_\infty U_\infty^3$)

Kn_R	$\alpha = 1$	$\alpha_t = 0.75$	$\alpha_n = 0.75$	$\alpha_r = 0.75$
0.04	0.162	0.157	0.165	0.162
2.00	0.641	0.455	0.681	0.663
(Calculated FM)	0.764	0.496	0.797	0.806

TABLE 1. Sharp cone, 6°

$M = 24.77, T_\infty = 11.69 \text{ K}, T_w = 375 \text{ K}$
 Incident mass flow rate (units of $\pi R^2 \rho_\infty U_\infty$)

Kn_R	$\alpha = 1$	$\alpha_t = 0.75$	$\alpha_n = 0.75$	$\alpha_r = 0.75$
0.0465	2.174	2.060	2.038	2.179
1.84	1.381	1.364	1.132	1.406
(Calculated FM)	1.191	1.191	1.191	1.191

Drag (units of $\frac{1}{2}\pi R^2 \rho_\infty U_\infty^2$)

Kn_R	$\alpha = 1$	$\alpha_t = 0.75$	$\alpha_n = 0.75$	$\alpha_r = 0.75$
0.0465	2.353	2.112	2.350	2.363
1.84	2.670	2.431	2.760	2.694
(Calculated FM)	2.866	2.675	3.435	2.866

Heat transfer rate (units of $\frac{1}{2}\pi R^2 \rho_\infty U_\infty^3$)

Kn_R	$\alpha = 1$	$\alpha_t = 0.75$	$\alpha_n = 0.75$	$\alpha_r = 0.75$
0.0465	0.549	0.508	0.521	0.539
1.84	0.830	0.783	0.619	0.850
(Calculated FM)	0.933	0.907	0.705	0.955

TABLE 2. Flat-faced cylinder

A tangential component of velocity of a single re-emitted molecule in a particular direction has a Gaussian or drifting Maxwellian probability distribution with mean velocity $1 - \sigma$ times the velocity before collision and temperature $\alpha_t T_w$, where T_w is the surface temperature. For the case where the distribution of tangential velocities of the incident molecules in a particular direction is itself a drifting Maxwellian with mean velocity V_1 and temperature T_1 , the distribution of tangential velocities of the re-emitted molecules in the same direction is a convolution of the two distributions, which has the same form but with mean velocity $V_r = (1 - \sigma) V_1$ and temperature $T_r = \alpha_t T_w + (1 - \alpha_t) T_1$. The model thus ensures that the distribution of tangential

velocity components is accommodated towards equilibrium with the surface, with accommodation coefficient σ for mean velocity and α_t for temperature.

In the C-L model, the magnitude of the normal component of velocity, u , behaves in the same way as the resultant magnitude of two orthogonal tangential components. It follows that the normal velocity component also accommodates towards equilibrium with the surface, although its distribution function is not Maxwellian but has the form

$$f(u) = A \exp\left(-\frac{u^2 + U_r^2}{2\mathcal{R}T_r}\right) I_0\left(\frac{uU_r}{\mathcal{R}T_r}\right),$$

where $U_r = -(1 - \alpha_n)^{1/2} U_i$, $T_r = \alpha_n T_w + (1 - \alpha_n) T_1$, A is a normalizing constant and I_0 is the modified Bessel function of order zero.

In the particular case where the velocity distribution of the incident molecules is a non-drifting Maxwellian at temperature T_1 , that of the re-emitted molecules has the form of a 'two-temperature' Maxwellian with different temperatures in the normal and tangential directions, the accommodation coefficients for the normal and tangential temperatures being α_n and α_t respectively and that for the kinetic energy of translation of the molecule being $\frac{1}{2}(\alpha_n + \alpha_t)$.

The resultant angular velocity of a molecule with two rotational degrees of freedom, such as nitrogen, can be treated in the same way as the normal velocity component or the resultant of the two tangential velocity components (Lord 1991). We use α_r to denote the accommodation coefficient for rotational kinetic energy.

3. Sharp slender cone

This type of flow has been studied by many workers. Bird (1985) used the flow over a 10° cone as a test case of a flow dominated by viscous rather than inertia forces, in order to investigate the sensitivity of his calculations to changes in molecular model and other Monte Carlo parameters. Dahlen & Brundin (1985) made drag measurements on cones of various half-angles, over a range of wall-to-stagnation temperature ratios, using magnetic suspension and balance techniques and Macrossan (1983) has carried out Monte Carlo simulations of their experiments, assuming complete surface accommodation. Legge & Dankert (1981) conducted an experimental investigation into the effects of incomplete surface accommodation on transition regime recovery factor, heat transfer and drag for cones with half-angles between 15° and 90° . When using nitrogen or air, they found drag coefficients for copper cones which were consistent with complete accommodation, but heat transfer was reduced when using cones with gold surfaces, particularly when the cone was cleaned and heated to 800 K.

In the present investigation, flow over a sharp 6° cone at a Mach number of 5.09 was simulated for a stagnation temperature to surface temperature ratio of 1.785, these conditions being typical of Dahlen & Brundin's experiments. Two different degrees of rarefaction were used, corresponding to Knudsen numbers, based on base radius, of 0.04 and 2.0.

The calculated global values of dimensionless incident mass flow rate, drag and heat transfer rate to the body are shown in table 1. These are presented as dimensionless quantities based on the free-stream mass flux $\rho_\infty U_\infty$, free-stream dynamic pressure $\frac{1}{2}\rho_\infty U_\infty^2$ and free-stream kinetic energy flux $\frac{1}{2}\rho_\infty U_\infty^3$ respectively. The area of the base of the cone πR^2 is used as the characteristic area. Results are shown for the case of complete accommodation and also for each of the three energy

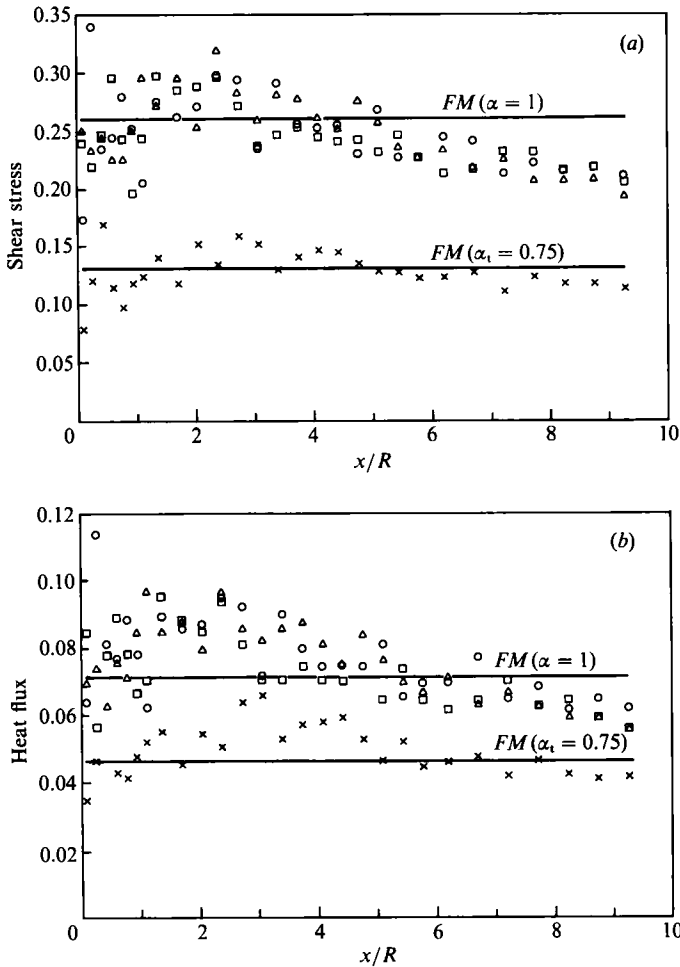


FIGURE 1. Sharp 6° cone, $M_\infty = 5.1$, $Kn_R = 2.0$. Longitudinal variation of surface properties: (a) shear stress, (b) heat flux. \square , complete accommodation; \times , $\alpha_t = 0.75$; \circ , $\alpha_n = 0.75$; \triangle , $\alpha_r = 0.75$; —, FM value.

accommodation coefficients reduced in turn to 0.75, the others remaining set at unity. Calculated free molecule values of the coefficients are also given. These were obtained by direct calculation using the properties of the C-L kernel mentioned previously, with the exception of the momentum and energy transfers due to the normal component of velocity of the reflected molecules; because the convolution integrals for these quantities with a drifting Maxwellian incident distribution are mathematically intractable, they were evaluated using a Monte Carlo technique.

In the rarefied case, reduction of α_t from 1 to 0.75 (corresponding to a value of σ of 0.5) leads to a 43% reduction in drag and a 30% reduction in heat transfer rate. The fractional changes in these quantities are thus of the same order as the changes in the corresponding accommodation coefficients and close to, but less than, the fractional changes which would be expected in free molecule flow (47% and 35% respectively). Effects of changes in α_n and α_r are small, as expected from the free molecule values, but in one case (α_n on drag) in the opposite sense. Even in the denser case, the reduction in α_t has a significant effect on the drag, producing a reduction of 23%, but it causes only a 3.4% reduction in heat transfer rate.

For the rarefied case, the variation with distance from the vertex of predicted surface shear stress and heat flux, again normalized by free-stream dynamic pressure and kinetic energy flux respectively, is shown in figures 1(a) and 1(b). Calculated free molecule values of these quantities for the cases of complete accommodation and of $\alpha_t = 0.75$ are shown also. Free molecule values for the other cases were found to be not significantly different from those for complete accommodation, which is perhaps not surprising in view of the fact that over the entire forward facing surface of the cone the tangential speed ratio is almost ten times the normal.

The Monte Carlo results appear to approach the correct free molecule limits at the cone vertex. As expected from the free molecule limits, the effects of incomplete accommodation appear to be restricted almost entirely to the value of α_t , mainly on shear stress but also, to a lesser extent, on heat flux.

Monte Carlo results for the incident mass flux and normal pressure are not shown, as these quantities demonstrate relatively little dependence on surface accommodation, even in free molecule flow.

4. Flat-faced circular cylinder

This flow has been investigated by Pullin, Davis & Harvey (1977) and by Davis *et al.* (1983), for the case of complete surface accommodation. In the former paper calculated values of near-axis flow properties and heat transfer to the front face, for a free-stream speed ratio of 8.36 and a wall-to-free stream temperature ratio of 3.15, are presented and the latter compared with the measurements of Metcalf, Coleman & Berry (1974). A simple inverse power law intermolecular potential was employed. Further measurements of heat transfer to the front face over a wide range of conditions have since been made by Coleman, Metcalf & Berry (1977). Davis *et al.* (1983) describe a series of simulations using three different molecular collision models. Near-axis profiles of density and translational and rotational temperature, for a free-stream Mach number of 24.77 and a wall-to-free stream temperature ratio of 32.1, are presented for the Morse potential, variable- ϕ model for several different degrees of rarefaction. Streamwise profiles of the same flow properties at different radii for all three models and a single set of flow conditions are also given and the density rotational temperature profile compared with the results of electron beam measurements.

In the present simulations, the flow conditions were chosen to coincide with those of Davis *et al.* at Knudsen numbers of 0.0465 and 1.84. The part of the surface of the cylinder included in the simulation consisted of the front face together with the curved surface up to seven radii downstream. The effects of changes in accommodation on the overall incident mass flow rate, drag and heat transfer rate on this surface are shown in table 2, together with the corresponding calculated free molecule values. These are normalized as for the cone, with the cross-sectional area πR^2 as the characteristic area. In the rarefied case, the drag is reduced by a reduction in α_t and increased by a reduction in α_n , as expected in the case of free molecule flow. However, the latter increase is only 3%, compared with 20% in the free molecule case. This is due mainly to the 18% reduction in incident mass flux in this case. Reduction in α_r produces a slight increase in drag, whereas no change would be expected in free molecule flow, but the change is probably within the error of the calculations. Reductions in α_t and α_n both cause reductions in heat transfer rate which are proportionally greater than in free molecule flow, the latter having the larger effect. A reduction in α_r produces a small increase in heat transfer rate, owing

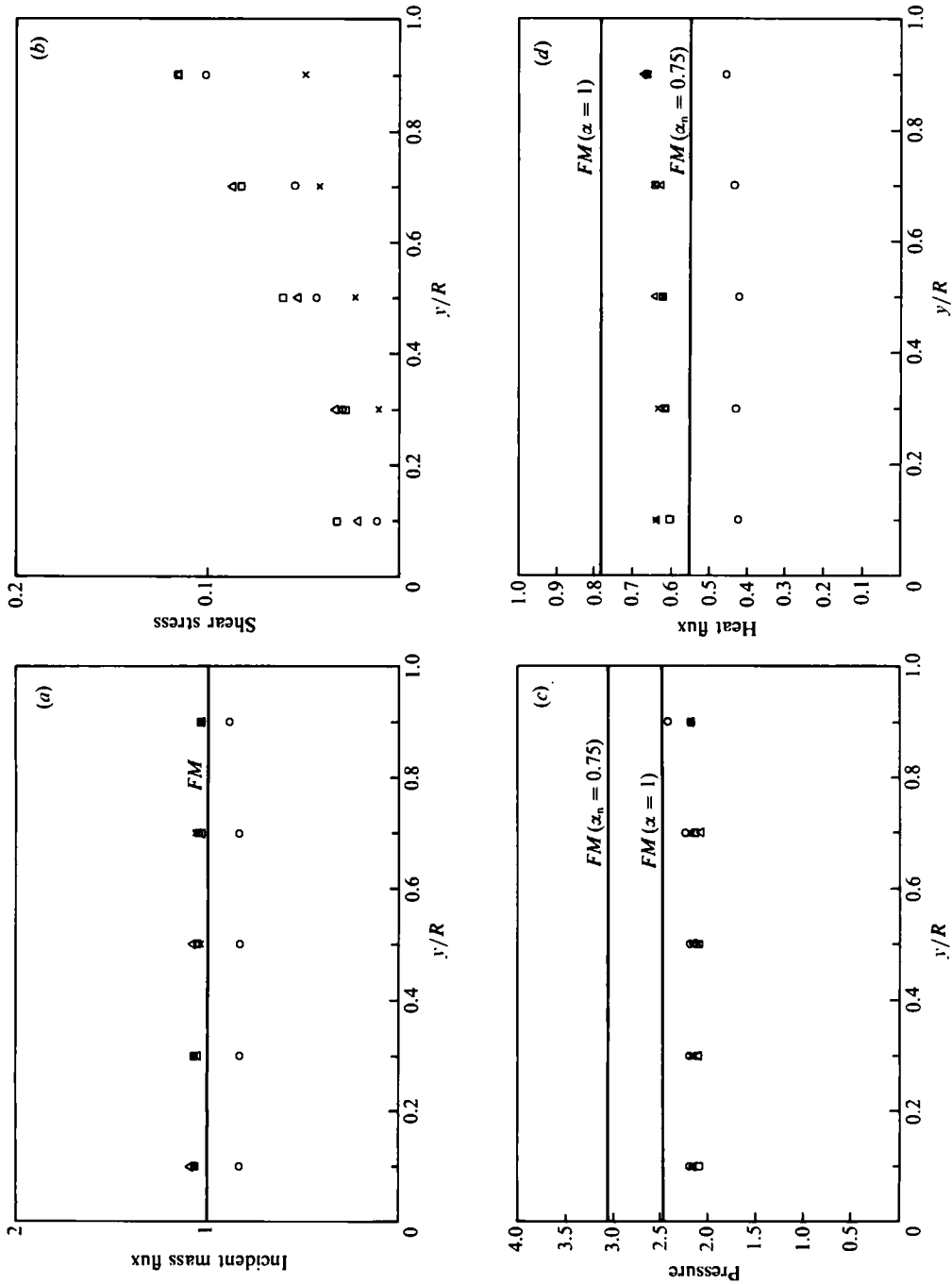


FIGURE 2. Flat faced cylinder, $M_\infty = 24.77$, $Kn_n = 1.84$. Radial variation of surface properties on front face: (a) incident mass flux, (b) shear stress, (c) normal pressure, (d) heat flux. For the key to symbols, see the caption to figure 1.

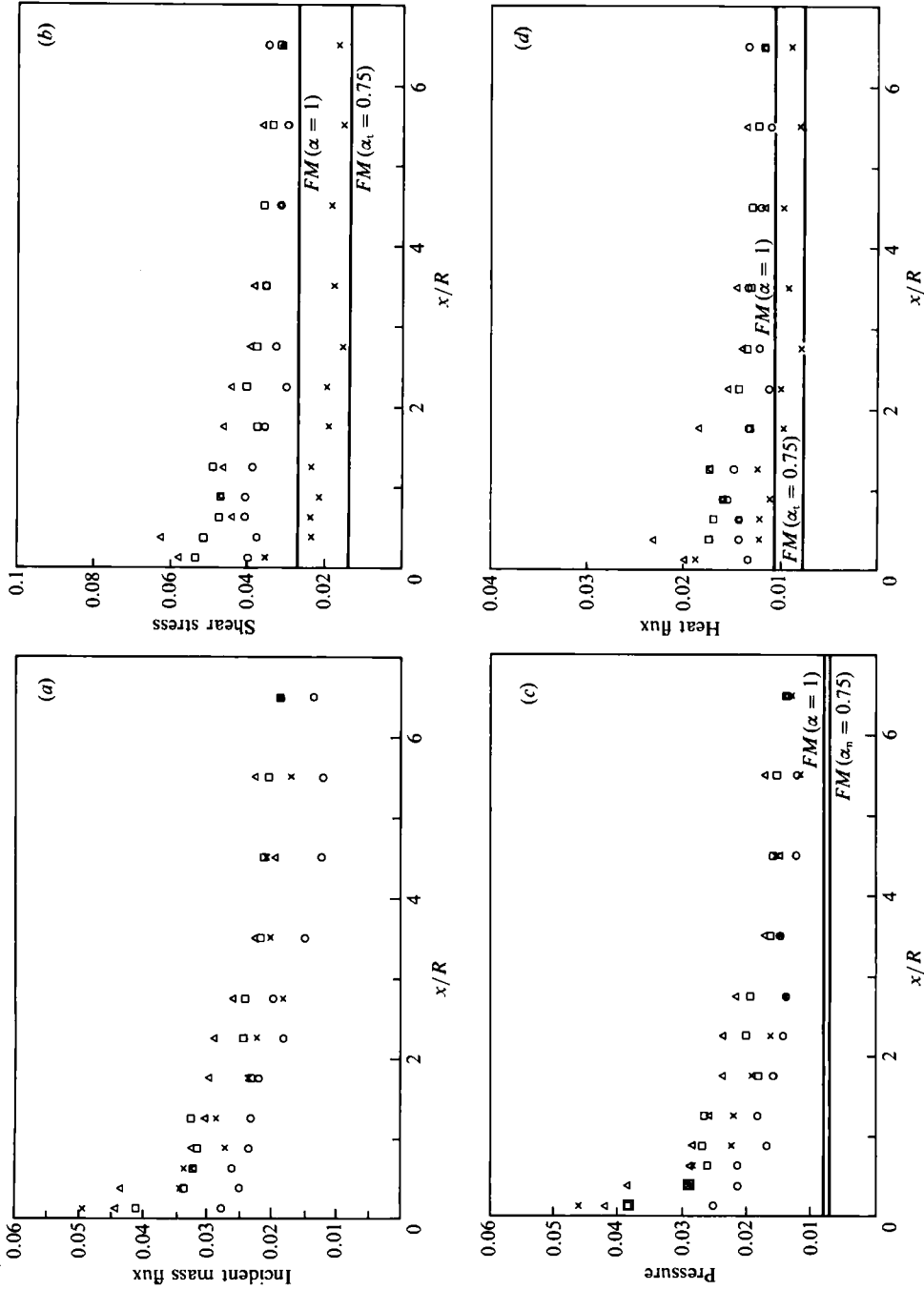


FIGURE 3. Flat faced cylinder, $M_\infty = 24.77$, $K\eta_R = 1.84$. Longitudinal variation of surface properties on curved surface: (a) incident mass flux, (b) shear stress, (c) normal pressure, (d) heat flux. For the key to symbols, see the caption to figure 1.

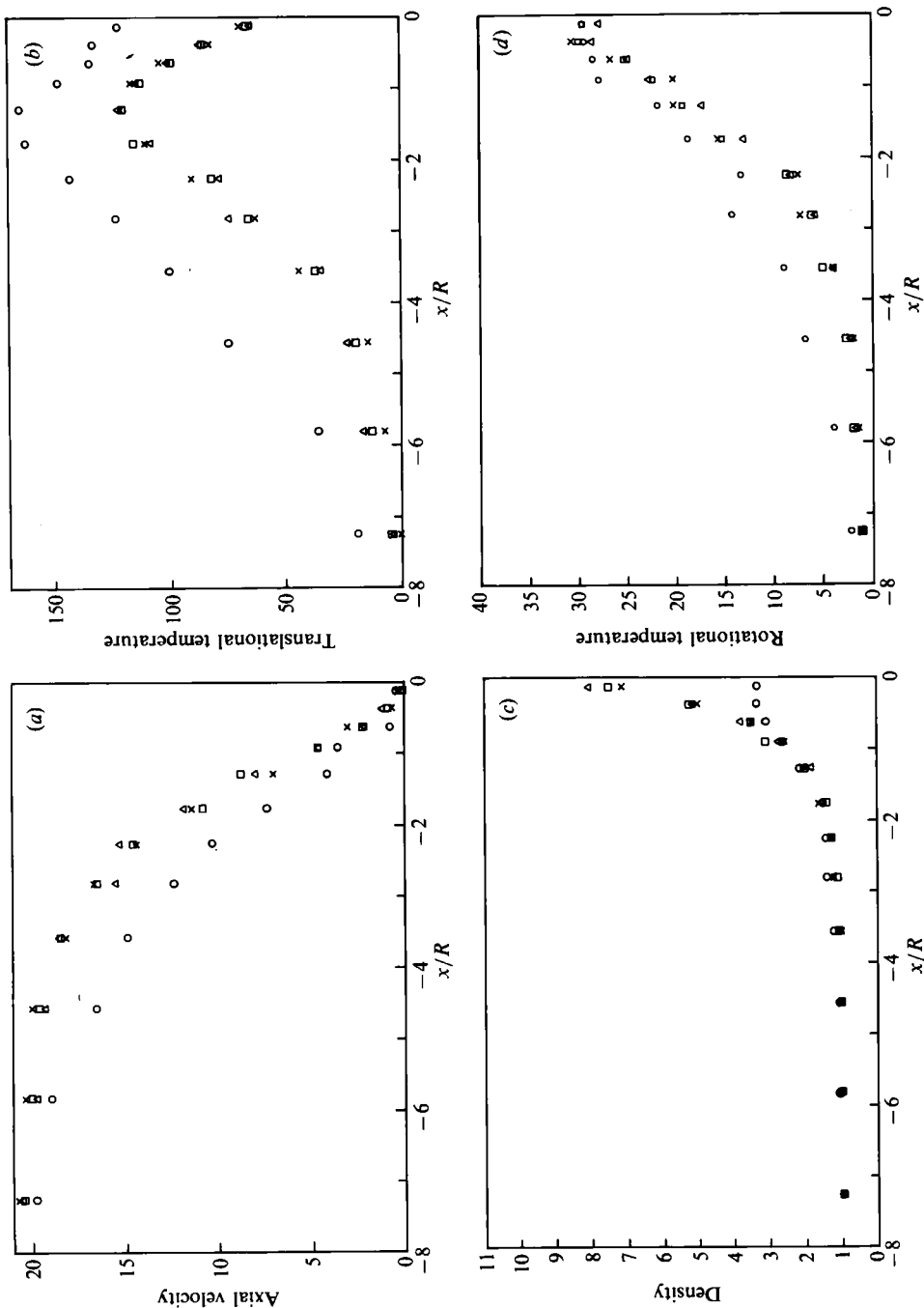


FIGURE 4. Flat faced cylinder, $M_\infty = 24.77$, $Kn_\infty = 1.84$. Near-axis variation of flow properties: (a) axial velocity, (b) translational temperature, (c) density, (d) rotational temperature. For the key to symbols, see the caption to figure 1.

to the fact that the rotational temperature of the gas near most of the surface is less than that of the surface, so that the surface is actually losing heat to the flow by means of rotational energy accommodation.

Figure 2 shows the radial variation across the front face of the cylinder of incident mass flux, shear stress, pressure and heat flux, normalized as for the cone, in the rarefied case. The incident mass flux shows a significant reduction for $\alpha_n = 0.75$, presumably owing to deflection of oncoming molecules away from the axis by collisions with molecules reflected from the front face. This leads to an even larger decrease in heat flux whereas the normal pressure is increased only slightly, despite the fact that normal momentum transfer in each surface collision is increased. The shear stress, on the other hand is affected more by α_t than α_n , although the effect of α_n is still noticeable.

Figure 3 shows the corresponding results for the cylindrical surface. Here most of the incident energy is associated with the tangential component of velocity and the heat flux is thus affected most by the value of α_t as, again, is the shear stress. The incident mass flux and the pressure are again more affected by α_n , although here the pressure decreases with α_n , because the mean normal velocity of the incident molecules is less than the value corresponding to the surface temperature.

Figure 4 shows the variation of axial velocity, translational temperature, density and rotational temperature normalized by their respective free-stream values, upstream of the cylinder along a line close to the axis, for the rarefied case. It is clear that all the upstream flow properties are drastically affected by the reduction in α_n . The axial velocity begins to reduce much further upstream and the density rises to only 3.5 times the free-stream value in the case $\alpha_n = 0.75$, compared to about 7.5 times in the other cases. The temperatures, including the rotational temperature, are also greatly increased. Contour maps of the whole flow field confirm that flow properties are affected by the reduction of α_n in all parts of the flow field. These effects may be attributed to the enhancement of flux and kinetic energy of the molecules re-emitted from the front face of the cylinder in the upstream direction owing to the reduction in α_n , bearing in mind that more than 99% of the total enthalpy of the free stream is due to axial kinetic energy and therefore, as far as the front face is concerned, contained in the normal component of velocity. These effects are insignificant in the less rarefied case (not shown).

5. Discussion

The effects of reduced surface accommodation of the translational kinetic energy due to the normal and tangential components of velocity have been shown to be significant, in the problems considered. The effects of reducing the accommodation of rotational kinetic energy appear to be less important. In general, it seems clear that, in order to make accurate predictions of the aerodynamic forces on, and heat transfer rates to, bodies in hypersonic rarefied flow it will be necessary to take surface accommodation into account. The Cercignani-Lampis model has been shown to be suitable for inclusion in direct-simulation Monte Carlo prediction codes and capable of a plausible description of rotational, as well as translational, energy accommodation.

The author is grateful to Professor J. K. Harvey of Imperial College, London, and to the Ministry of Defence, for permission to use the direct simulation Monte Carlo program developed by them.

REFERENCES

- BABOVSKY, H., GROPENGIESSER, F., NEUNZERT, H. & STRUCKMEIER, J. 1989 Low-discrepancy methods for the Boltzmann equation. In *Rarefied Gas Dynamics, 16th Symp.* (ed. E. P. Muntz, D. P. Weaver & D. H. Campbell), vol. 118, p. 85. AIAA.
- BIRD, G. A. 1976 *Molecular Gas Dynamics*. Clarendon.
- BIRD, G. A. 1985 Hypersonic flow past a slender cone. In *Rarefied Gas Dynamics, 13th Symp.* (ed. O. M. Belotserkovskii, M. N. Kogan, S. S. Kutateladze & A. K. Rebrov), vol. 1, p. 349. Plenum.
- BOYD, I. D. 1990 Rotational-translation energy transfer in rarefied nonequilibrium flows. *Phys. Fluids A2*, 447.
- BOYD, I. D. 1991 Monte Carlo study of vibrational relaxation processes. In *Rarefied Gas Dynamics, 17th Symp.* (ed. A. E. Beylich), p. 793. VCH, Weinheim, Germany.
- CERCIGNANI, C. 1971 Models for gas-surface interactions: comparison between theory and experiment. In *Rarefied Gas Dynamics, 7th Symp.* (ed. D. Dini), vol. 1, p. 75. Editrice Technico Scientifica.
- CERCIGNANI, C. & LAMPIS, M. 1971 Kinetic models for gas-surface interactions. *Transport Theory Stat. Phys.* 1, 101.
- CERCIGNANI, C. & FREZZOTTI, A. 1989 Numerical simulation of supersonic rarefied gas flows past a flat plate: effects of the gas-surface interaction model on the flowfield. In *Rarefied Gas Dynamics, 16th Symp.* (ed. E. P. Muntz, D. P. Weaver & D. H. Campbell), vol. 118, p. 552. AIAA.
- COLEMAN, G. T., METCALF, S. C. & BERRY, C. J. 1977 Heat transfer to hemisphere cylinders and bluff cylinders between continuum and free molecular limits. In *Rarefied Gas Dynamics, 10th Symp.* (ed. J. L. Potter), vol. 51, part 1, p. 393. AIAA.
- DAHLEN, G. A. & BRUNDIN, C. L. 1985 Wall temperature effects on rarefied hypersonic cone drag. In *Rarefied Gas Dynamics, 13th Symp.* (ed. O. M. Belotserkovskii, M. N. Kogan, S. S. Kutateladze and A. K. Rebrov), vol. 1, p. 453. Plenum.
- DAVIS, J., DOMINY, R. G., HARVEY, J. K. & MACROSSAN, M. N. 1983 An evaluation of some collision models used for Monte Carlo calculations of diatomic rarefied hypersonic flows. *J. Fluid Mech.* 135, 355.
- HARVEY, J. K. 1989 Inelastic collision models for Monte Carlo simulation computation. In *Rarefied Gas Dynamics, 16th Symp.* (ed. E. P. Muntz, D. P. Weaver & D. H. Campbell), vol. 117, p. 3. AIAA.
- KUSCER, I. 1971 Reciprocity in scattering of gas molecules by surfaces. *Surface Sci.* 25, 225.
- KUSCER, I. 1974 Phenomenology of gas-surface accommodation. In *Rarefied Gas Dynamics, 9th Symp.* (ed. M. Becker & M. Fiebig), vol. 2, Paper E1. DFVLR Press, Porz-Wahn, Germany.
- LEGGE, H. & DANKERT, C. 1981 Influence of incomplete accommodation in wind tunnel experiments on heat transfer and drag of sharp cones in the transition regime. In *Rarefied Gas Dynamics, 12th Symp.* (ed. S. S. Fisher), vol. 74, Part 2, p. 964. AIAA.
- LORD, R. G. 1991 Application of the Cercignani-Lampis scattering kernel to direct simulation Monte Carlo calculations. In *Rarefied Gas Dynamics, 17th Symp.* (ed. A. E. Beylich), p. 1427. VCH, Weinheim, Germany.
- MACROSSAN, M. N. 1983 Diatomic collision models used in the Monte Carlo direct simulation method applied to rarefied hypersonic flows. PhD thesis, Department of Aeronautics, Imperial College, University of London.
- MARRIOTT, P. & HARVEY, J. K. 1991 New approach for modelling energy exchange and chemical reactions in the direct simulation Monte Carlo method. In *Rarefied Gas Dynamics, 17th Symp.* (ed. A. E. Beylich), p. 784. VCH, Weinheim, Germany.
- METCALF, S. C., COLEMAN, G. T. & BERRY, C. J. 1974 Heat transfer to bluff faced and hemispherical faced cylinders between continuum and free molecular flow limits. In *Rarefied Gas Dynamics, 9th Symp.* (ed. M. Becker & M. Fiebig), vol. 2, Paper D16. DFVLR Press, Porz-Wahn, Germany.
- PULLIN, D. I., DAVIS, J. & HARVEY, J. K. 1977 Monte Carlo calculations of the rarefied transition flow past a bluff faced cylinder. In *Rarefied Gas Dynamics, 10th Symp.* (ed. J. L. Potter), vol. 51, Part 1, p. 379. AIAA.